Report

Current Biology

Integrin-Mediated Adhesion in the Unicellular Holozoan *Capsaspora owczarzaki*

Highlights

- *C. owczarzaki* adheres to surfaces using actin-dependent filopodia
- Integrin β2 and vinculin localize as distinct patches in the filopodia
- Cell adhesion and integrin localization are enhanced by mammalian fibronectin
- Integrin-β2-blocking antibody reduces cell adhesion on fibronectin-coated surfaces

Authors

Helena Parra-Acero, Matija Harcet, Núria Sánchez-Pons, Elena Casacuberta, Nicholas H. Brown, Omaya Dudin, Iñaki Ruiz-Trillo

Correspondence

omaya.dudin@epfl.ch (O.D.), inaki.ruiz@multicellgenome.org (I.R.-T.)

In Brief

Parra-Acero et al. investigate cell-substrate adhesion in the filasterean *C. owczarzaki*, a close unicellular relative of animals. They show that cell adhesion relies on actin-dependent filopodia and is mediated by the integrin adhesome. This suggests that the role of integrins in cell-matrix adhesion was established before the emergence of animals.

Parra-Acero et al., 2020, Current Biology *30*, 1–6
November 2, 2020
https://doi.org/10.1016/j.cub.2020.08.015

CellPress

Please cite this article in press as: Parra-Acero et al., Integrin-Mediated Adhesion in the Unicellular Holozoan *Capsaspora owczarzaki*, Current Biology (2020), https://doi.org/10.1016/j.cub.2020.08.015

Current Biology

CellPress
OPEN ACCESS

Report

Integrin-Mediated Adhesion in the Unicellular Holozoan *Capsaspora owczarzaki*

Helena Parra-Acero,[1] Matija Harcet,[1,2] Núria Sánchez-Pons,[1] Elena Casacuberta,[1] Nicholas H. Brown,[3] Omaya Dudin,[1,4,*] and Iñaki Ruiz-Trillo[1,5,6,7,*]

[1]Institut de Biologia Evolutiva (CSIC-Universitat Pompeu Fabra), Passeig Marítim de la Barceloneta 37-49, 08003 Barcelona, Catalonia, Spain
[2]Laboratory for Molecular Genetics, Division of Molecular Biology, Ruđer Bošković Institute, Zagreb, Croatia
[3]Department of Physiology, Development and Neuroscience, University of Cambridge, Cambridge CB2 3DY, UK
[4]Swiss Institute for Experimental Cancer Research (ISREC), School of Life Sciences, Swiss Federal Institute of Technology Lausanne (EPFL), 1015 Lausanne, Switzerland
[5]Departament de Genètica, Microbiologia i Estadística, Universitat de Barcelona, Av. Diagonal, 645, 08028 Barcelona, Catalonia, Spain
[6]ICREA, Passeig Lluís Companys 23, 08010 Barcelona, Catalonia, Spain
[7]Lead Contact
*Correspondence: omaya.dudin@epfl.ch (O.D.), inaki.ruiz@multicellgenome.org (I.R.-T.)
https://doi.org/10.1016/j.cub.2020.08.015

SUMMARY

In animals, cell-matrix adhesions are essential for cell migration, tissue organization, and differentiation, which have central roles in embryonic development [1–6]. Integrins are the major cell surface adhesion receptors mediating cell-matrix adhesion in animals. They are heterodimeric transmembrane proteins that bind extracellular matrix (ECM) molecules on one side and connect to the actin cytoskeleton on the other [7]. Given the importance of integrin-mediated cell-matrix adhesion in development of multicellular animals, it is of interest to discover when and how this machinery arose during evolution. Comparative genomic analyses have shown that core components of the integrin adhesome pre-date the emergence of animals [8–11]; however, whether it mediates cell adhesion in non-metazoan taxa remains unknown. Here, we investigate cell-substrate adhesion in *Capsaspora owczarzaki*, the closest unicellular relative of animals with the most complete integrin adhesome [11, 12]. Previous work described that the life cycle of *C. owczarzaki* (hereafter, *Capsaspora*) includes three distinct life stages: adherent; cystic; and aggregative [13]. Using an adhesion assay, we show that, during the adherent life stage, *C. owczarzaki* adheres to surfaces using actin-dependent filopodia. We show that integrin β2 and its associated protein vinculin localize as distinct patches in the filopodia. We also demonstrate that substrate adhesion and integrin localization are enhanced by mammalian fibronectin. Finally, using a specific antibody for integrin β2, we inhibited cell adhesion to a fibronectin-coated surface. Our results suggest that adhesion to the substrate in *C. owczarzaki* is mediated by integrins. We thus propose that integrin-mediated adhesion pre-dates the emergence of animals.

RESULTS AND DISCUSSION

Exponentially growing *Capsaspora* are thought to be in an adherent life stage consisting of single cells adhering to the substrate (Figure 1) [13]. However, the capacity of *Capsaspora* to adhere to a surface has never been systematically investigated. To achieve this, we modified previously published adhesion assays [14, 15] (Figure 2A). Briefly, we seeded exponentially growing cells into an untreated multi-well plate and let them sit for 2.5 h. We then discarded the cells remaining in suspension and fixed the remaining cells attached to the bottom of the well. After several washes, we indirectly measured the number of cells that remained adhered to the surface by quantifying DAPI staining of nucleic acids (Figure 2A; STAR Methods). Using this assay, we observed that fluorescence intensity increased with cell concentration (Figures 2B and 2C). This assay is most sensitive between 1.6×10^6 cells/mL and 6.6×10^6 cells/mL (Figure 2C), so we seeded 3.3×10^6 cell/mL for all future experiments to allow us to measure with confidence any increase or decrease in cell adhesion. Our results show that *Capsaspora* can adhere to surfaces and the adherent cells are quantitatively measured with our assay.

Initial descriptions of *Capsaspora* showed that it has dynamic filopodia [17], and a recent study revealed that these filopodia contact the substrate and appear to hold the cell body above the surface [18]. We examined filopodia behavior in live cells by performing time-lapse microscopy of adherent *Capsaspora* cells transfected with a membrane marker (NMM-mCherry) [18]. We observed that filopodia not only hold the cell over the surface but appear to actively participate in its motility (Figure 2D; Video S1). This suggests that filopodia are the major interactor with the surface and thus potentially crucial for cell-surface adhesion. In animals, filopodia formation and maintenance relies extensively on the actin cytoskeleton [19, 20]. Several actin regulators involved in filopodia formation, including Arp2/3 complex, a major actin nucleator in animals [20, 21], are found in

Please cite this article in press as: Parra-Acero et al., Integrin-Mediated Adhesion in the Unicellular Holozoan *Capsaspora owczarzaki*, Current Biology (2020), https://doi.org/10.1016/j.cub.2020.08.015

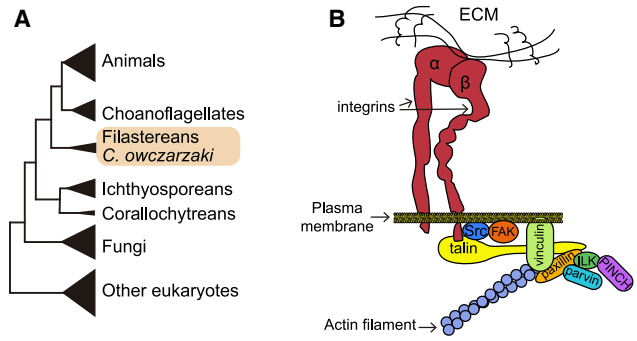

Figure 1. Phylogenetic Position of *Capsaspora owczarzaki* and Illustrative Summary of the Animal Integrin Adhesome

(A) Phylogenetic position of *Capsaspora owczarzaki* in the tree of life (adapted from [16]).

(B) Schematic drawing of the integrin adhesion complex in animals (adapted from [11]).

Capsaspora [22]. We thus used latrunculin A (LatA), a general inhibitor of actin polymerization, and Arp2/3-specific inhibitor CK-666 to assess the role of filopodia in adhesion [23, 24]. We observed that LatA-treated cells were round and lacked both filopodia and actin filaments (Figure 2E). CK-666-treated cells did not lack actin filaments and maintained an elongated cell shape but completely lacked filopodia (Figure 2E). Adhesion assays of LatA and CK-666-treated cells showed a substantial decrease in adhesion (Figure 2F). Despite the potential toxic effect of pharmacological inhibitors, this result suggests that cell-surface adhesion in *Capsaspora* could be mediated by Arp2/3-dependent filopodia.

In animals, cell-matrix adhesions are formed by the interaction of integrins and cytoplasmic integrin-associated proteins, such as vinculin, at discrete sites in the cell [25–29]. To address whether conserved components of the integrin adhesome in *Capsaspora* are also involved in cell adhesion, we developed antibodies for immuno-localization. We successfully obtained functional antibodies against both the cysteine-rich region of integrin β2 (anti-β2E3) and vinculin (Figure S1; Data S1). The integrin β2 is the most highly expressed of the four *Capsaspora* β subunits, contributing 68% and 73% of the beta subunit mRNA fragments per kilobase of transcript per million (FPKM) at adherent and aggregative stages [13]. We observed that both antibodies stain the cell body and multiple distinct patches along filopodia (Figures 3A, 3B, and S2A). Antibodies staining of the cell body included distinct patches at the cell surface and more diffused localization at the cell body, which might represent vesicular trafficking of both integrin and vinculin (Figures S2A and S2D). To avoid contrast issues due to the high fluorescence intensity of the antibodies in the cell body (Figures S2A and S2D), we chose to show and focus our attention to integrin β2 and vinculin patches in the filopodia. Co-immunostaining showed a partial overlap and some patches contain both, whereas others have just one of the proteins (Figures 3C and S2B). This incomplete co-localization could either indicate the dynamic localization of both proteins or imply distinctive and independent roles of both proteins. This last idea is reinforced with the knowledge that choanoflagellates lack integrins but still comprise vinculin [11, 12, 30]. Nonetheless, taken together, these results suggest that the integrin and vinculin patches may represent anchorage sites of adhesion.

To further investigate that, we first assessed whether *Capsaspora* adheres preferentially to any of the well-known integrin ECM ligands in animals, namely fibronectin, laminin, and collagen 1 [31–33]. Coating the plastic substrate with bovine serum albumin (BSA) reaching up to 40 mg/mL reduced the adhesion of *Capsaspora* by ~70% (Figures 3D and S2C). This suggests that a protein secreted by *Capsaspora* sticks to the plastic substrate and provides a ligand for adhesion, and the binding of this protein to the plastic substrate is reduced by prior coating with BSA. Notably, the remaining ~30% of adherent cells at highest BSA concentration might be non-specifically attached to the plastic substrate. Similar to BSA, coating the plastic substrate with mammalian laminin or collagen reduced the adhesion of *Capsaspora* (Figures 3D and S2C). In contrast, mammalian fibronectin increases cell adhesion with increasing concentration reaching up to 20 μg/mL (Figures 3D and S2C). This indicates that *Capsaspora* can use mammalian fibronectin as a substrate for cell adhesion. We then assessed whether adhesion to mammalian fibronectin affects filopodia morphology or localization of integrin β2 and vinculin to the filopodia. The number of filopodia as well as their length increased (Figures 3E–3G). The overall fluorescence intensity of integrin β2 and vinculin staining within filopodia increased (Figures 3H and 3I), and the overall distribution remained similar, with a patchy appearance (data not shown). These results suggest that mammalian fibronectin promotes cell adhesion by increasing the number and length of filopodia as well as by promoting recruitment of integrin and vinculin to the filopodia. *Capsaspora* does not have an ortholog of fibronectin but does have secreted proteins with the tripeptide Arg-Gly-Asp (RGD) sequences, which are candidates for endogenous ligands. Purifying integrin ligands from *Capsaspora* in the future would improve our understanding of the physiological role of cell adhesion in *Capsaspora*.

Finally, to directly assess the role of the β2 integrin cell-substrate adhesion, we generated a new antibody to the β2 integrin subunit, this time targeting the ligand-binding β-I domain (anti-β2GP1; Figure S1). Pre-incubation of cells with this antibody prior to plating, substantially reduced adhesion to fibronectin-treated surfaces (Figure 3J). In contrast, pre-incubation with the antibody against the cysteine-rich stalk slightly impaired adhesion (Figure 3J). This suggests that β2 integrin interacts with mammalian fibronectin to achieve cell attachment. Whether such interaction is normally mediated by *Capsaspora*'s RGD-domain-containing proteins or secreted proteins from *Capsaspora*'s host organism *Biomphalaria glabrata* is still to be determined.

Taken together, these results show that the major integrin β subunit in *Capsaspora* makes a substantial contribution to substrate adhesion. The localization of integrin β2 and vinculin in discrete patches within the filopodia suggests that these structures contribute to cell-substrate adhesion, which is an unexpected role for integrin adhesion within filopodia. In animal cells, filopodia are more generally associated with dynamic exploration of the substrate rather than forming stable adherent contacts. Our findings provide further support to the view that integrin-mediated cell adhesion evolved before animals emerged. Further investigation of integrin-mediated adhesion in

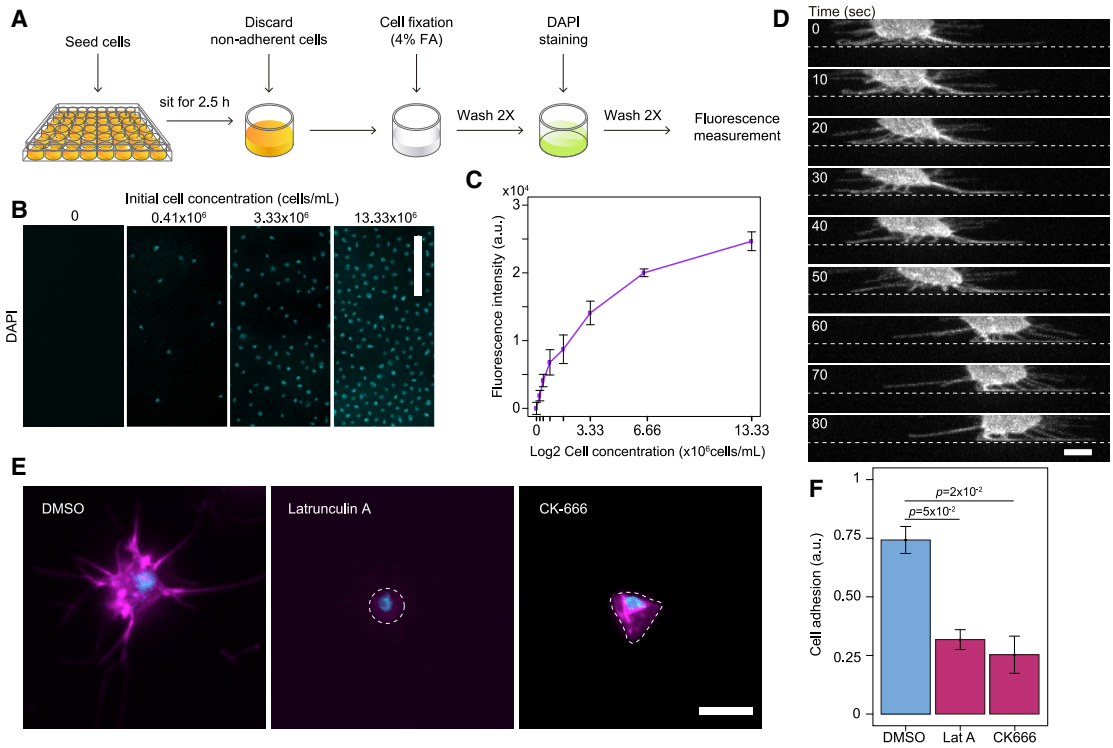

Figure 2. *Capsaspora owczarzaki* Adheres to Surfaces Using Actin-Dependent Filopodia

(A) Protocol for measuring cell adhesion in *Capsaspora*.

(B) DAPI-stained cells remaining attached to the surface following the adhesion assay. Number of seeded cells at the beginning of the assay is indicated. Scale bar, 50 μm.

(C) Fluorescence intensity measures of an adhesion assay performed with increasing concentration of *Capsaspora* cells seeded on untreated plates.

(D) Time lapse of an adherent *Capsaspora* cell transfected with a membrane label (CoNMM:mCherry). Images were taken as a z stack every 10 s. A maximum intensity projection of an orthogonal view is represented. Punctate line marks the substrate. Scale bar, 5 μm. See also Video S1.

(E) Phalloidin (magenta) and DAPI (cyan) staining of floating cells from an adhesion assay treated with 0.05 mM LatA or 0.1 mM CK666 and its corresponding DMSO control. Scale bar, 5 μm.

(F) Adhesion assay in presence of drugs. Data represent the ratio of signal from adherent cells treated with Lat A, CK666, or DMSO relative to the signal of untreated cells. Bars represent mean ± SEM (n = 3) of three independent experiments. As both DMSO controls show similar effect, only one is shown for simplicity. p values from a paired t test are shown.

Capsaspora, particularly during the aggregative stage, by examining its ligands and intracellular binding partners will shed more light into the origins of the integrin-mediated adhesion and its role in the evolution of animal multicellularity.

STAR★METHODS

Detailed methods are provided in the online version of this paper and include the following:

- KEY RESOURCES TABLE
- RESOURCE AVAILABILITY
  - Lead Contact
  - Materials Availability
  - Data and Code Availability
- EXPERIMENTAL MODEL AND SUBJECT DETAILS
- METHOD DETAILS
  - Custom polyclonal antibodies design
  - Protein extraction
  - Western Blot
  - Immunoprecipitation and Mass-spectrometry
  - Membrane labeling
  - Adhesion assay
  - Immunolocalization of adhesome proteins
  - Microscopy
- QUANTIFICATION AND STATISTICAL ANALYSIS
  - Image analysis
  - Statistical Analysis

SUPPLEMENTAL INFORMATION

Supplemental Information can be found online at https://doi.org/10.1016/j.cub.2020.08.015.

ACKNOWLEDGMENTS

We thank Meritxell Antó for technical support. We thank Núria Ros-Rocher for assistance with transfection of the organism. We acknowledge the Biomolecular Screening and Protein Technologies Unit from CRG (Barcelona, Spain) for assistance with antibody production as well as the CRG/UPF Proteomics Unit for proteomics analysis. We also thank CRG Advanced Light Microscopy Unit for support with confocal imaging. We also thank the many other people

Please cite this article in press as: Parra-Acero et al., Integrin-Mediated Adhesion in the Unicellular Holozoan *Capsaspora owczarzaki*, Current Biology (2020), https://doi.org/10.1016/j.cub.2020.08.015

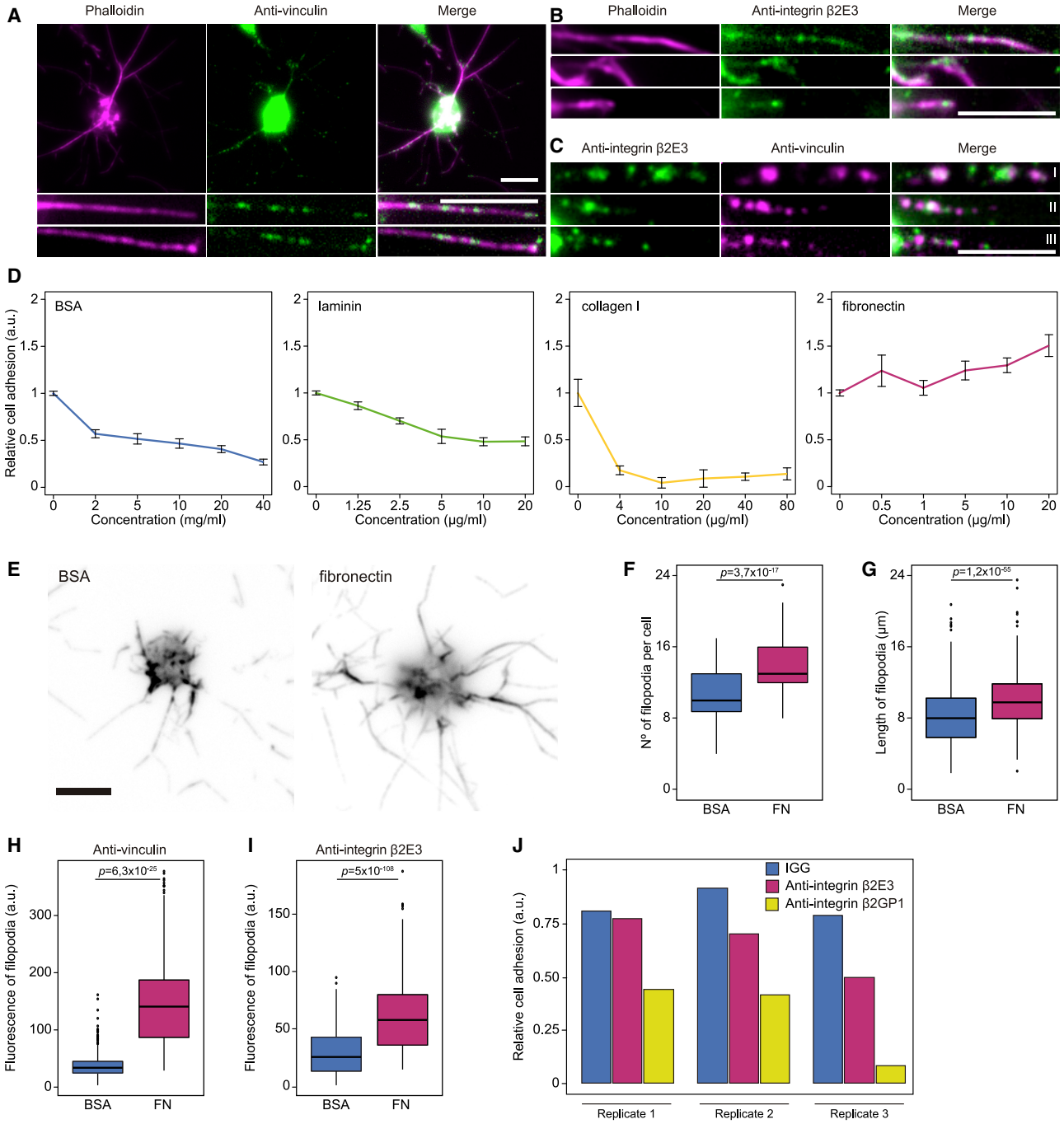

Figure 3. *Capsaspora owczarzaki* Undergoes Integrin-Mediated Cell Adhesion on Fibronectin-Coated Surfaces

(A) Immunostaining of adherent and phalloidin-stained *Capsaspora* cells (magenta) with anti-vinculin antibody (green). Distinct patches of vinculin are observed in the filopodia. Scale bar, 5 μm.

(B) Immunostaining of adherent and phalloidin-stained *Capsaspora* cells (magenta) with antibody for integrin β2 subunit, anti-β2E3 (green). Distinct patches of integrin β2 are observed in the filopodia. Scale bar, 5 μm.

(C) Co-immunostaining of vinculin (magenta) with integrin β2 (green). Scale bar, 5 μm.

(D) Cell adhesion measurements on surfaces treated with increasing concentrations of bovine serum albumin (BSA), laminin, collagen I, and fibronectin. BSA was included as a control. Relative cell adhesion was set as the ratio between the signal obtained between ligand-coated and uncoated surfaces. Data represent the mean ± SEM of 4 technical replicates.

(E) Phalloidin-stained cells seeded on either fibronectin- or BSA-treated coverslips. Scale bar, 5 μm.

(F) Number of filopodia per cell seeded on either fibronectin- or BSA-treated coverslips (n = 164). p value from a Mann-Whitney test is shown.

(G) Filopodia length of cells seeded on either fibronectin- or BSA-treated coverslips (n = 500). p value from a Mann-Whitney test is shown.

(legend continued on next page)

who have worked in our lab and who have provided support and feedback over the years. This work was funded by European Research Council Consolidator Grant (ERC-2012-Co-616960) to I.R.-T.; O.D. was supported by a Swiss National Science Foundation Early PostDoc Mobility fellowship (P2LAP3_171815) and a Marie Sklodowska-Curie individual fellowship (MSCA-IF 746044). M.H. received funding from the People Programme (Marie Curie Actions) of the European Union's Seventh Framework Programme FP7/2007-2013/ under REA grant agreement no. 330925. N.H.B.'s work on this project was supported by a Royal Society International Exchange Grant (IE141189). The CRG/UPF Proteomics Unit is part of the of Proteored, PRB3 and is supported by grant PT17/0019 of the PE I+D+i 2013-2016, funded by ISCIII and ERDF.

AUTHOR CONTRIBUTIONS

H.P.-A., M.H., O.D., and I.R.-T. designed the study and set up the methodology. H.P.-A. and O.D. performed the adhesion assays, the microscopy, and the chemical inhibition experiments. N.S.-P., H.P.-A., and M.H. designed and validated the antibodies. N.H.B. and E.C. assisted in the design of the project and analysis of results. I.R.-T. and O.D. provided supervision. H.P.-A. and O.D. wrote the original draft. All authors reviewed and edited the manuscript.

DECLARATION OF INTERESTS

The authors declare no competing interests.

Received: April 27, 2020
Revised: June 29, 2020
Accepted: August 4, 2020
Published: August 27, 2020

REFERENCES

1. Berrier, A.L., and Yamada, K.M. (2007). Cell-matrix adhesion. J. Cell. Physiol. *213*, 565–573.
2. Bulgakova, N.A., Klapholz, B., and Brown, N.H. (2012). Cell adhesion in Drosophila: versatility of cadherin and integrin complexes during development. Curr. Opin. Cell Biol. *24*, 702–712.
3. Hynes, R.O. (1999). Cell adhesion: old and new questions. Trends Cell Biol. *9*, M33–M37.
4. Hynes, R.O., and Zhao, Q. (2000). The evolution of cell adhesion. J. Cell Biol. *150*, F89–F96.
5. Maartens, A.P., and Brown, N.H. (2015). Anchors and signals: the diverse roles of integrins in development. Curr. Top. Dev. Biol. *112*, 233–272.
6. Winograd-Katz, S.E., Fässler, R., Geiger, B., and Legate, K.R. (2014). The integrin adhesome: from genes and proteins to human disease. Nat. Rev. Mol. Cell Biol. *15*, 273–288.
7. Hynes, R.O. (2002). Integrins: bidirectional, allosteric signaling machines. Cell *110*, 673–687.
8. Brown, M.W., Sharpe, S.C., Silberman, J.D., Heiss, A.A., Lang, B.F., Simpson, A.G.B., and Roger, A.J. (2013). Phylogenomics demonstrates that breviate flagellates are related to opisthokonts and apusomonads. Proc. Biol. Sci. *280*, 20131755.
9. de Mendoza, A., Suga, H., Permanyer, J., Irimia, M., and Ruiz-Trillo, I. (2015). Complex transcriptional regulation and independent evolution of fungal-like traits in a relative of animals. eLife *4*, e08904.
10. Hehenberger, E., Tikhonenkov, D.V., Kolisko, M., Del Campo, J., Esaulov, A.S., Mylnikov, A.P., and Keeling, P.J. (2017). Novel predators reshape holozoan phylogeny and reveal the presence of a two-component signaling system in the ancestor of animals. Curr. Biol. *27*, 2043–2050.e6.
11. Sebé-Pedrós, A., and Ruiz-Trillo, I. (2010). Integrin-mediated adhesion complex: cooption of signaling systems at the dawn of Metazoa. Commun. Integr. Biol. *3*, 475–477.
12. Sebé-Pedrós, A., Roger, A.J., Lang, F.B., King, N., and Ruiz-Trillo, I. (2010). Ancient origin of the integrin-mediated adhesion and signaling machinery. Proc. Natl. Acad. Sci. USA *107*, 10142–10147.
13. Sebé-Pedrós, A., Irimia, M., Del Campo, J., Parra-Acero, H., Russ, C., Nusbaum, C., Blencowe, B.J., and Ruiz-Trillo, I. (2013). Regulated aggregative multicellularity in a close unicellular relative of metazoa. eLife *2*, e01287.
14. Pierschbacher, M.D., and Ruoslahti, E. (1984). Cell attachment activity of fibronectin can be duplicated by small synthetic fragments of the molecule. Nature *309*, 30–33.
15. Busk, M., Pytela, R., and Sheppard, D. (1992). Characterization of the integrin alpha v beta 6 as a fibronectin-binding protein. J. Biol. Chem. *267*, 5790–5796.
16. Torruella, G., de Mendoza, A., Grau-Bové, X., Antó, M., Chaplin, M.A., del Campo, J., Eme, L., Pérez-Cordón, G., Whipps, C.M., Nichols, K.M., et al. (2015). Phylogenomics reveals convergent evolution of lifestyles in close relatives of animals and fungi. Curr. Biol. *25*, 2404–2410.
17. Stibbs, H.H., Owczarzak, A., Bayne, C.J., and DeWan, P. (1979). Schistosome sporocyst-killing Amoebae isolated from Biomphalaria glabrata. J. Invertebr. Pathol. *33*, 159–170.
18. Parra-Acero, H., Ros-Rocher, N., Perez-Posada, A., Kożyczkowska, A., Sánchez-Pons, N., Nakata, A., Suga, H., Najle, S.R., and Ruiz-Trillo, I. (2018). Transfection of *Capsaspora owczarzaki*, a close unicellular relative of animals. Development *145*, 1–8.
19. Mattila, P.K., and Lappalainen, P. (2008). Filopodia: molecular architecture and cellular functions. Nat. Rev. Mol. Cell Biol. *9*, 446–454.
20. Mellor, H. (2010). The role of formins in filopodia formation. Biochim. Biophys. Acta *1803*, 191–200.
21. Rottner, K., Faix, J., Bogdan, S., Linder, S., and Kerkhoff, E. (2017). Actin assembly mechanisms at a glance. J. Cell Sci. *130*, 3427–3435.
22. Sebé-Pedrós, A., Burkhardt, P., Sánchez-Pons, N., Fairclough, S.R., Lang, B.F., King, N., and Ruiz-Trillo, I. (2013). Insights into the origin of metazoan filopodia and microvilli. Mol. Biol. Evol. *30*, 2013–2023.
23. Yarmola, E.G., Somasundaram, T., Boring, T.A., Spector, I., and Bubb, M.R. (2000). Actin-latrunculin A structure and function. Differential modulation of actin-binding protein function by latrunculin A. J. Biol. Chem. *275*, 28120–28127.
24. Burke, T.A., Christensen, J.R., Barone, E., Suarez, C., Sirotkin, V., and Kovar, D.R. (2014). Homeostatic actin cytoskeleton networks are regulated by assembly factor competition for monomers. Curr. Biol. *24*, 579–585.
25. Zamir, E., and Geiger, B. (2001). Components of cell-matrix adhesions. J. Cell Sci. *114*, 3577–3579.
26. Kanchanawong, P., Shtengel, G., Pasapera, A.M., Ramko, E.B., Davidson, M.W., Hess, H.F., and Waterman, C.M. (2010). Nanoscale architecture of integrin-based cell adhesions. Nature *468*, 580–584.
27. Green, H.J., and Brown, N.H. (2019). Integrin intracellular machinery in action. Exp. Cell Res. *378*, 226–231.

(H) Vinculin fluorescence intensity of filopodia (n > 100) from cells seeded on either fibronectin- or BSA-treated coverslips. p value from a Mann-Whitney test is shown.
(I) Integrin β2 fluorescence intensity of filopodia (n > 100) from cells seeded on either fibronectin- or BSA-treated coverslips. p value from a Mann-Whitney test is shown.
(J) Cell adhesion of *Capsaspora* on fibronectin-coated surfaces in presence of 20 μg/mL of control immunoglobulin G (IgG), anti-β2E3, and anti-β2GP1 antibodies. Relative cell adhesion was set as the ratio of signal obtained between cells treated with integrin antibodies and their corresponding buffers. Three independent replicates are shown.
See also Figures S1 and S2.

28. Bays, J.L., and DeMali, K.A. (2017). Vinculin in cell-cell and cell-matrix adhesions. Cell. Mol. Life Sci. *74*, 2999–3009.

29. Klapholz, B., and Brown, N.H. (2017). Talin - the master of integrin adhesions. J. Cell Sci. *130*, 2435–2446.

30. Miller, P.W., Pokutta, S., Mitchell, J.M., Chodaparambil, J.V., Clarke, D.N., Nelson, W.J., Weis, W.I., and Nichols, S.A. (2018). Analysis of a vinculin homolog in a sponge (phylum Porifera) reveals that vertebrate-like cell adhesions emerged early in animal evolution. J. Biol. Chem. *293*, 11674–11686.

31. Humphries, J.D., Byron, A., and Humphries, M.J. (2006). Integrin ligands at a glance. J. Cell Sci. *119*, 3901–3903.

32. Campbell, I.D., and Humphries, M.J. (2011). Integrin structure, activation, and interactions. Cold Spring Harb. Perspect. Biol. *3*, a004994.

33. Barczyk, M., Carracedo, S., and Gullberg, D. (2010). Integrins. Cell Tissue Res. *339*, 269–280.

34. Schneider, C.A., Rasband, W.S., and Eliceiri, K.W. (2012). NIH Image to ImageJ: 25 years of image analysis. Nat. Methods *9*, 671–675.

35. Yamada, K.M., and Kennedy, D.W. (1984). Dualistic nature of adhesive protein function: fibronectin and its biologically active peptide fragments can autoinhibit fibronectin function. J. Cell Biol. *99*, 29–36.

36. Bourdon, M.A., and Ruoslahti, E. (1989). Tenascin mediates cell attachment through an RGD-dependent receptor. J. Cell Biol. *108*, 1149–1155.

37. Weinreb, P.H., Simon, K.J., Rayhorn, P., Yang, W.J., Leone, D.R., Dolinski, B.M., Pearse, B.R., Yokota, Y., Kawakatsu, H., Atakilit, A., et al. (2004). Function-blocking integrin alphavbeta6 monoclonal antibodies: distinct ligand-mimetic and nonligand-mimetic classes. J. Biol. Chem. *279*, 17875–17887.

38. Schindelin, J., Arganda-Carreras, I., Frise, E., et al. (2012). Fiji: an open-source platform for biological-image analysis. Nat. Methods *9*, 676–682.

Please cite this article in press as: Parra-Acero et al., Integrin-Mediated Adhesion in the Unicellular Holozoan *Capsaspora owczarzaki*, Current Biology (2020), https://doi.org/10.1016/j.cub.2020.08.015

CellPress
OPEN ACCESS

STAR★METHODS

KEY RESOURCES TABLE

REAGENT or RESOURCE	SOURCE	IDENTIFIER
Antibodies		
C. owczarzaki integrin β2E3	this paper	N/A
C. owczarzaki integrin β2GP1	this paper	N/A
C. owczarzaki vinculin	this paper	N/A
anti-guinea pig HRP	Invitrogen	Cat# 61-4620
anti-rat HRP	Abcam	Cat# ab7097
guinea-pig IgG	MBL	Cat# PM067
rat IgG	Sigma-Aldrich	Cat# I8015
anti-guinea pig Dylight 488	Thermo Scientific	Cat# SA5-10094
anti-rat Alexa 488	Invitrogen	Cat# A-11006
Chemicals, Peptides, and Recombinant Proteins		
Bacto Peptone	GIBCO	Cat# 211677
Bacto Yeast Extract	GIBCO	Cat# 212750
Yeast nucleic acid (Ribonucleic Acid, Type VI from Torula Yeast)	Sigma-Aldrich	Cat# R-6625
Folic acid	Sigma-Aldrich	Cat# F8758
Hemin	Sigma-Aldrich	Cat# H9039
Fetal bovine serum (heat-inactivated)	Sigma-Aldrich	Cat# F9665
KH_2PO_4	Sigma-Aldrich	Cat# P5655
Na_2HPO_4	Sigma-Aldrich	Cat# S5136
cOmplete ULTRA Tablets, Mini, EDTA-free, EASYpack Protease Inhibitor Cocktail	Sigma-Aldrich	Cat# 4693159001
Tris-Glycine-SDS Buffer	Sigma-Aldrich	Cat# T777
DAPI	Sigma-Aldrich	Cat# 10236276001
Latrunculin A	Sigma-Aldrich	Cat# L5163
CK-666	Sigma-Aldrich	Cat# SML0006
Fibronectin	Sigma-Aldrich	Cat# F1141
Laminin	Sigma-Aldrich	Cat# L2020
Collagen I	Sigma-Aldrich	Cat# A3294
BSA	Sigma-Aldrich	Cat# SML0006
Phalloidin-Texas red	Invitrogen	Cat# T7471
Phalloidin-Alexa 350	Invitrogen	Cat# A22281
Phalloidin-Alexa 546	Invitrogen	Cat# A22283
Experimental Models: Organisms/Strains		
Capsaspora owczarzaki	Iñaki Ruiz-Trillo's lab; originally described in [17]	strain ATCC®30864
Software and Algorithms		
ImageJ	[34]	https://imagej.nih.gov/ij/
Other		
Nitrocellulose membrane	Amersham	Cat# 10600004
Precast 4-20% acrylamide gel	BioRad	Cat# 456-1094
Protein A-conjugated beads	Merck Millipore	Cat# LSKMAGA10
Protein G-conjugated beads	Merck Millipore	Cat# LSKMAGG10
μ-Slide 4-well glass-bottom dish	Ibidi	Cat# 80427

Please cite this article in press as: Parra-Acero et al., Integrin-Mediated Adhesion in the Unicellular Holozoan *Capsaspora owczarzaki*, Current Biology (2020), https://doi.org/10.1016/j.cub.2020.08.015

RESOURCE AVAILABILITY

Lead Contact

Further information and requests for resources and reagents should be directed to and will be fulfilled by the Lead Contact, Iñaki Ruiz-Trillo (inaki.ruiz@multicellgenome.org).

Materials Availability

Antibodies generated in this study will be made available upon request, but will be limited due to small amounts.

Data and Code Availability

This study did not generate any unique datasets or code.

EXPERIMENTAL MODEL AND SUBJECT DETAILS

Capsaspora owczarzaki cell cultures (strain ATCC®30864) were grown axenically at 23°C in ATCC medium 1034 (modified PYNFH medium). 25 cm^2 and 75 cm^2 flasks were used for culture (Falcon®, #353108 and #353136 respectively). Adherent cells were obtained by growing cells for few days and before floating cells appeared.

METHOD DETAILS

Custom polyclonal antibodies design

β2E3-antigen was designed as a region in the stalk of the extracellular domain of the integrin β2 (CAOG_05058, amino acid region 733-835). The sequence (5′ CAATGCGTCTGCGATGCTTTGCACGCCGGCCCTGCTTGCGGCTGCGTCAAGGGTGTCTGCCC CTCTGTTGGCGGCGTTCGCTGCAATGGCGGTGATTGCGACCCAATCTGCGGTATCTGCACTTGCCCGCCTGGCAAGACTGGACC TGCGTGCGACTGCGATACTGTTGCTCACCCGTGCCCGACTGGCAACTCCACCTCTGGCGTTGTGCTTCCCTGCTCTGGCCAAGG CACGTGCCTGCAGTCGTCTGCCACTCAGTGCGGCATCTGCTTGTGCAACCGTGATCCGCTGACTGGCACGCCGCTGTAC 3′) corresponding to that region was amplified using the following primers: forward (5′ CTGAATTCCAATGCGTCTGCGATGC 3′) and reverse (5′ AGACTCGAGGTACAGCGGCGTG 3′) and cloned into plasmid pGEx4T1 using *EcoR*I and *Xho*I restriction enzymes (this plasmid contains a GST-tag to facilitate expression and purification). The polypeptide was produced in *E.coli* by the Biomolecular Screening and Protein Technologies (BSM&PT) Unit of CRG, Barcelona; and its corresponding polyclonal antibody was produced in guinea-pig by TebuBio and affinity purified by BSM&PT, CRG. β2GP1-antigen is a polypeptide corresponding to a region in the β-I domain of integrin β2 (amino acid region 100-403, sequence: VPQTVSIVVTIPQRKEVEFFYLFDLSGSMGD DLRNVKNLGNNLRDKMQSLCRGSSSISSDCHYWRLGSHVDRPNGPFGGSGDYEFRIEGIASGDDRSFGSFGAFSTALGNAATEWGND FPESQYSSMLQSLLCVNWNPARRHILLLATDATGHMEFDSNRLSSATAFPQRRALQKCHVTPGTASSSSNFANTINAATLDHEIPSWPQ IKAAFLDKNVVPILAITAYSSNNDHYDSFINALGFGGRAGLSGDSSNVLSVIESVYNQIVGTIKPQLFDNGMDKFVRSLTPAAGYTGLSRG DSRTFT). The vinculin-antigen is a polypeptide corresponding to the C terminus region of one of the vinculin homologs (CAOG_05123, amino acid region 335-834, sequence: LAERIKANPSDEVAQARFAELMDELPRELRLLEKALADDAIHAQMAVFANV AEPLSAIVQAAQSGNAADVNAAGVELQSQTATLVKASRTVASNAPDSEVSKEINTLSKQLEDLVPQIVVAARLVAANPDDQAARANLDLL MKSWDSKVARLNELSEQVAQPHAFLEVAERTIAAEVAKAKAAVTAQDKPSFDKAVKNIKATAARAGRLAAAEEKNTDDADFRKKMAERR ARIEASINGLEPTMNKAFTSRNAADIDAAVQPVTSSVSELKKEIAQSQGIEASGSGSGAGAAGAGSSQAGSASSTAIANEVRKSEEKQVA EIAAAAGVSPQAVASHPISIAAGNLKLVASRWDAKNNALVQAADKISEKMRTMAAFSMQPNNKKDMIDMAKSMASEVAEIVKLAKAAAE QCSDRRLKANLLQLCDKIPTISTQLRIIASVKAANPSDSDAETQLIAGSKNLMDVVTEIVKGTEAASLKSFSSVASTANVALQWKRKALGH). Antigens for both β2GP1 and vinculin, and their corresponding polyclonal antibodies (in guinea-pig and rat respectively) were designed and produced by Genecust. Both antibodies were affinity-purified by Genecust. Antibody stock concentration were: anti-β2E3 1.8 mg/mL, anti-vinculin and anti-β2GP1 1mg/mL.

Protein extraction

Protein extraction was performed as follows: adherent and exponentially growing cells were scraped and pelleted at 5000 x g. Cells were then washed once with PBS 1X and kept at either −20°C or −80°C. Cells were resuspended in lysis buffer (Tris-HCl 50mM pH 8.8, NaCl 150mM, SDS 0.1%, EDTA 5mM, EGTA 1mM, NP-40 1%, MgCl2 1mM, CaCl2 1mM, DTT 1mM, PMSF 0.5mM, half cOmplete (4693159001, Sigma-Aldrich) for 3mL buffer) and kept on ice for 10 min before being sonicated (amplitude 10%, 3 pulses of 15 s, 45 s between pulses). To obtain the final protein extract was obtained after centrifugation for 30 min at 20,000 x g at 4°C and the supernatant was kept as the soluble fraction.

Western Blot

For SDS-PAGE, 1-5 μg of purified antigen or 20 μg protein extract were loaded in a precast 4%–20% acrylamide gel (BioRad 456-1094). Gels were run for the first 20-30 min at 40V, later at 80-100V. Proteins and antigens were wet-transferred in TGS 1X (Sigma T7777-1L) with methanol 20% to a nitrocellulose membrane (Amersham 10600004) at 20-30 V 4°C overnight. After transfer, membranes were incubated with blocking solution (Tween 0.1% and 5% no-fat powder milk in PBS 1X) at room temperature (RT) for 1

Please cite this article in press as: Parra-Acero et al., Integrin-Mediated Adhesion in the Unicellular Holozoan *Capsaspora owczarzaki*, Current Biology (2020), https://doi.org/10.1016/j.cub.2020.08.015

hour. Membranes with protein extract were quickly washed with 0.1% Tween in PBS 1X (PBS-T hereafter), and incubated with primary antibodies at 4°C overnight in the following conditions: anti-IntB2E3 3.6 μg/mL in PBS-T with 1% milk, anti-IntB2GP1 and anti-vinculin 2μg/mL in PBS-T. Membranes with antigens were incubated with primary antibody 2h at RT in the following conditions: anti-β2E3 1.8μg/mL in PBS-T with 1% milk (no-fat, powder), anti-β2GP1 and anti-vinculin 1μg/mL in PBS-T. After incubation, membranes were washed 4 times with PBS-T and incubated with secondary antibodies: anti-guinea pig HRP (Invitrogen, #61-4620), and anti-rat HRP (Abcam, ab7097) at 0.1μg/mL in PBS-T for 3 h (2 h for antigens) at RT. After incubation with secondary antibody, membranes were washed again with PBS-T. Detection was performed by chemiluminescence (SuperSignalTM West Pico Chemiluminescent Substrate 34078 Thermofisher).

Immunoprecipitation and Mass-spectrometry

For immunoprecipitation (IP), protein extraction was performed as previously described, in lysis buffer without DTT or SDS, and 1% Triton x100 instead of NP-40. 1 mg of protein extract was used for IP with vinculin antibody and 1.5mg for IP with the β2E3 and β2GP1 antibodies. For IP with guinea-pig antibody protein A-conjugated magnetic beads (Merck Millipore, LSKMAGA10) were used. For IP with rat antibody, protein G-magnetic beads (Merck Millipore, LSKMAGG10) were used instead. The lysate was pre-cleared by incubating with 50μL of beads per condition overnight at 4°C. Beads were previously washed twice with IP-buffer (PBS-Tween 0.1%). Additionally, 50uL beads per antibody were washed with IP-buffer and blocked with blocking solution (1%BSA in PBS-Tween 0.1%) for 1h at room temperature. Blocked beads were mixed with a dilution of each antibody in IP-buffer (9μg/mL of anti-β2E3 and 5μg/mL of anti-β2GP1 and anti-vinculin) and incubated 4h at 4°C, then washed three times with IP-buffer. Pre-cleared lysate was mixed with antibody-bound beads and incubated overnight at 4°C. Beads were then washed with IP-buffer three times and kept without liquid at −20°C. Negative controls with guinea-pig IgG (MBL PM067) and rat IgG (Sigma, I8015) (5μg/mL) were made following the same procedure. "In-beads" digestion and Mass Spectrometry was performed in the CRG/UPF Proteomics Unit in Barcelona, Spain. See results in Data S1.

Membrane labeling

Capsaspora was transfected in its adherent stage according to a calcium phosphate precipitation method (Parra-Acero et al., 2018) with the *CoNMM:mcherry* construct, which directs mCherry to the cell membrane, (Parra-Acero et al., 2018). Transfected cells were seeded in a μ-Slide 4-well glass-bottom dish (Ibidi, #80427) and grown overnight at 23°C prior to imaging.

Adhesion assay

Adherent cells were obtained as mentioned above and then scraped and harvested by centrifugation at 5000 x g before being re-suspended in growth medium without fetal bovine serum (FBS) (FBS presence showed heterogeneous results, data not shown). Cells were then seeded in untreated 48-well plate (32048, SPL Life Sciences) at a concentration of 3.3 x10^6 cells/ml. Cells were left to sit and adhere for 2.5 hours at 23°C. The medium containing floating cells, was then gently removed and adherent cells were fixed with 4% formaldehyde for 10 min at room temperature (RT). The wells containing fixed cells were washed once with 1X PBS and stained with DAPI (50 μg/ml) for (Roche, 10236276001) 10 min at RT and protected from light. Finally, wells were washed 3 times with 1X PBS followed by immediate fluorescence measurement with a plate reader (TECAN infinite 200). Fluorescence of DAPI (350nm excitation /470nm emission) was read using the i-control™ Microplate Reader Software. Detection was performed from the top, set to 5x5 reads per well (circle filled) and gain was set to "optimal" automatically by the software for each independent experiment. Unless pointed otherwise, four technical replicates were performed for each condition per experiment. During analysis, background signal was removed. For easier visualization of the results, fluorescence measurements were normalized to the control of seeded cells in untreated wells. Equal number of cells adhering in uncoated and coated wells or treated and untreated cells would set a value equal to 1.

For assessing the role of actin in cell-surface adhesion, both Latrunculin A (LatA) (Sigma-Aldrich L5163-100UG) and CK-666 (SML0006-5MG) were used as pharmacological inhibitors. Stock solutions was 20mM for LatA and 10mM for CK-666 in DMSO. Re-suspended cells were incubated for 10 minutes with both pharmacological inhibitors at a final concentration of 50 μM of LatA and 100 μM of CK666, and its corresponding DMSO amount as control. Then, cells were plated and the treatment continued during the sitting time. Adhesion assay was then preformed as mentioned above.

For ECM-ligand affinity measurements, untreated multi-well plates were coated with different concentration of fibronectin (Sigma F1141-2MG), laminin (Sigma L2020-1MG), collagen I (Sigma C3867-1VL) or BSA (Sigma A3294-10G). BSA was included as control as it acts as a blocking agent of unspecific adhesion sites [15, 35–37]. For all proteins, solutions of the desired concentration were prepared by diluting the stock solutions in PBS 1X. Fibronectin-coated plates were incubated overnight at 4°C and washed once with PBS 1X before plating the cells. Laminin-coated plates were incubated 2 hours at 37°C and washed 3 times with PBS 1X before plating the cells. Collagen I-coated and BSA-coated plates were incubated 1 hour at room temperature (18°C culture room) and washed once with PBS1X before plating the cells.

For assessing role of integrin inhibition using competition with anti-integrin antibodies anti-β2E3 and anti-β2GP1 as well as the control guinea-pig IgG antibody (MBL PM067) were diluted in medium without FBS and mixed with re-suspended cells, to reach a final concentration of 20 μg/mL for each antibody. Then, cells mixed with antibodies were seeded on a fibronectin-coated plate (20 μg/ml). Negative controls were prepared by replacing antibodies with corresponding buffer as such (IgG: PBS + 50% Glycerol Buffer, anti-β2E3: PBS + 20% Glycerol, anti-β2GP1: Water). Three independent technical replicates were performed. Each replicate represents

Please cite this article in press as: Parra-Acero et al., Integrin-Mediated Adhesion in the Unicellular Holozoan *Capsaspora owczarzaki*, Current Biology (2020), https://doi.org/10.1016/j.cub.2020.08.015

the mean of four internal replicates for each condition. Fluorescence measurements were normalized to the control of seeded cells in presence of above-mentioned corresponding buffers). Furthermore, two commercially available integrin inhibitors; peptide RGDS (Sigma A9041) and peptide RGQS (Sigma A5686), were tested at a final concentration of 2mM and plated with cells on fibronectin coated plates without success (data not shown).

Immunolocalization of adhesome proteins

Coverslips used for immunostaining were previously coated with either BSA 4% or Fibronectin at 20 μg/mL and incubated overnight at 4°C prior to being washed once with PBS1X. Cells were scraped from a confluent culture and resuspended in growth medium without FBS before being added over the coated coverslips inside a 6 well/plate and incubated at 23°C for 2.5 hours. Excess liquid was then removed before fixing the cells with 4% formaldehyde (in PBS1X) for 10 min at RT. Cells were then washed with PBS 1X and incubated 2h at RT with primary antibodies diluted in blocking solution (1% BSA, 0.1% Triton in PBS 1X) at the following concentrations: anti-β2E3 (9 μg/mL), anti-vinculin (10 μg/mL). Cells were washed with blocking solution (once quick, twice for 10 min) and incubated 1 hour at RT with secondary antibodies diluted in blocking solution as follows: anti-guinea pig Dylight 488 (Thermo Scientific, SA5-10094) (0.5 μg/mL) and anti-rat Alexa 488 (Invitrogen, A-11006) (1 μg/mL). Cells were washed with PBS 1X and incubated with phalloidin-Texas red (Invitrogen T7471) (1:100 from stock, equals 2 units/mL) 15 min in darkness. They were mounted on glass slides with ProlonGold (Invitrogen, P36930). Negative controls lacking primary antibody were performed in the same conditions and used to adjust the imaging settings.

For co-immunostaining, cells were incubated at the same time with anti-β2E3 (9 μg/mL) and anti-vinculin (10 μg/mL). Secondary antibodies used were anti-guinea pig Dylight 488 (at 0.5 μg/mL) and anti-rat Texas red (1 μg/mL). Cells were finally stained with phalloidin Alexa 350 (Invitrogen A22281) (2 units/mL) for 15 min at RT.

For actin localization, cells treated with Lat A (0.05mM) and CK666 (0.1 mM) and DMSO were fixed adding 4% formaldehyde directly in the medium for 10 min. Cells were then pelleted by repeated centrifugations of 5 min at 3000 g, where the liquid was carefully removed. Cells were washed with PBS 1X and stained with Phalloidin Alexa 546 (Invitrogen A22283) (2 units/mL) and DAPI (10 μg/mL) for 15min in darkness at RT.

Microscopy

Images of fixed cells were obtained using a Zeiss Axio Observer Z.1 Epifluorescence inverted microscope equipped with Colibri LED illumination system and an Axiocam 503 mono camera using a Plan-Apochromat 63X/1.4 oil objective. Confocal microscopy of the transfected cell was obtained using an Andor Revolution XD imaging system equipped with a Olympus inverted microscope, using a 60x oil objective, a spinning disk scanhead (Yokogawa CSU-X1) and an Andor Ixon 897E Dual Mode EM-CCD camera. Images were edited using Fiji Imaging Software (version 2.0.0-rc-44/1.50e) [38].

QUANTIFICATION AND STATISTICAL ANALYSIS

Image analysis

Image analysis was done using ImageJ software (version 1.52) [34]. For measurements of number and length of filopodia we used the ObjectJ plugin in ImageJ and measured the filopodia from the surface plane of fixed cells images. Only filopodia connected to the cell body were counted (filopodia that were broken during the staining procedure were ignored). The mean fluorescence intensity of integrin and vinculin antibody staining was measured along manually selected filopodia (over 100 filopodia). This was achieved using a segmented line selection covering the width and the whole length of the filopodia (excluding the cell body) which was then used to measure the mean fluorescence intensity. Fluorescence intensity was corrected for background fluorescence and normalized to the length of the corresponding filopodium. Similarly, the method was used to measure only the length of filopodia when seeded on either BSA or Fibronectin (Figure 3G). For fluorescence intensity profiles of integrin β2 and vinculin co-immunostaining along filopodia (Figure S2B), a segmented line (width = 10) was drown along the length of filopodia and a plot profile was generated using imageJ function for both integrin β2 and vinculin signal independently. Fluorescence values were then normalized to maximum value after correcting background fluorescence.

Statistical Analysis

Results from drug effect and antibody on adhesion assay are shown as mean ± standard error of the mean (s.e.m) as from 3 independent experiments. The significance of difference in the mean was tested using the parametric t test for paired samples. Results from measurements on morphology of filopodia and intensity of IAPs staining are represented as box-plots. The significance for each condition on the measurements was tested using the non-parametric Mann-Whitney U test (Wilcoxon Rank-Sum test) for independent samples. All statistical analyses were performed using the R Stats Package version 3.3.1.